Time Encoding of Bandlimited Signals, an Overview *

Aurel A. Lazar, Ernő K. Simonyi and László T. Tóth

November 5, 2005

Abstract

Time encoding is a real-time, asynchronous mechanism for encoding the amplitude information of an analog bandlimited signal into a time sequence, or time codes, based on which the signal can be reconstructed. Time codes can be generated by simple nonlinear asynchronous analog circuits with low power consumption. The circuits generating the time codes and the procedures carrying out the reconstruction are referred to as Time Encoding Machines (TEMs) and Time Decoding Machines (TDMs), respectively. We give an overview of this novel information representation modality.

1 Introduction

A fundamental question in information processing is how to represent an analog signal, $x(t)$, by a discrete sequence. If $x(t)$ is bandlimited to $[-\Omega, \Omega]$, then the classical sampling theorem [25, 45] uses the uniformly-taken amplitude samples $x(kT)$ to represent $x(t)$ as

$$x(t) = \frac{\pi}{\Omega} \sum_{k \in \mathbb{Z}} x(kT) g(t - kT) \quad \text{for} \quad T \leq \frac{\pi}{\Omega}, \tag{1}$$

where

$$g(t) = \frac{\sin \Omega t}{\pi t} \tag{2}$$

is the impulse response of an ideal lowpass filter (LPF) with cutoff frequency Ω and $\mathbb{Z}$ is the set of integers. Uniform sampling naturally calls for synchronous implementations. A typical scenario is shown in Figure 1(a) where a common clock operates the analog-to-digital converter (ADC) and the digital signal processor (DSP). As this solution has been used over decades, the art of conventional discrete-time (DT) and digital signal processing is very well developed. Insensitivity to noise and analog imperfections such as circuit tolerances and component matching are well-known characteristics of synchronous systems. A major

*BNET Technical Report #5-05, Department of Electrical Engineering, Columbia University, New York, NY, October 2005. Proceedings of the Conference on Telecommunication Systems, Modeling and Analysis, Dallas, TX, November 17-20, 2005, to appear.

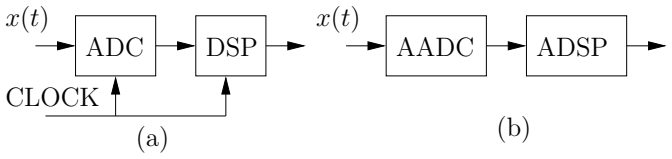

Figure 1: Synchronous (a) and asynchronous (b) signal processing.

limitation of Systems on Chip implementations is the large power consumption due to the high-frequency clock employed [16]. The use of lower supply voltages for both analog and digital signal processing [28] has reduced the power requirements of these systems. Concurrently, the use of oversampling techniques is typically employed in synchronous ADC implementations (as in, e.g., sigma-delta modulation [40]). Higher clock frequency, however, increases the electromagnetic interference (EMI) on supply rails that in turn corrupts the analog input signal hence the overall conversion [15]. Alternative solutions for a number of applications have been investigated [42].

Motivated by the success of asynchronous design of digital logic circuits impressive research is underway in the area of asynchronous ADCs (AADCs) [24, 23, 7, 15, 20, 43], and asynchronous digital signal processors (ADSPs) [36, 10, 37, 47]. Although this research is still in an initial phase, faster average conversion and metastability-free conversion under low power have already been demonstrated. As shown in Fig. 1(b), these systems use no clock. They are often referred to as time-based systems, since timing information is used to carry and forward information. This is illustrated by a quantizer as one of the simplest level-crossing type of AADC in Figure 2. As shown, the irregularly spaced times, t_k, are defined at the transitions of the quantizer output, $z(t)$.

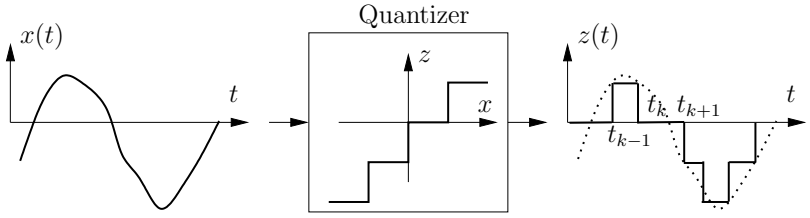

Figure 2: Quantizer as one of the simplest AADC.

2 TEM-TDM Processing

Only a small number of papers on asynchronous digital signal processing investigated time-based systems as information representation and processing modalities. For example, can the times t_k of Figure 2 be used for a loss-free characterization of $x(t)$? Or equivalently, is it possible to reconstruct $x(t)$ based on these t_k's if certain conditions are met? The methods used in irregular sampling help in answering these questions.

2.1 Irregular sampling

Researchers have long been fascinated of how uniform sampling can be used in practice. Starting from early achievements [9], substantial results have been accumulated over the years both in theory [48, 19] and efficient numerical solutions [11, 12], just to mention a few. In particular, in terms of certain times, t_k, and the corresponding amplitude values, $x(t_k)$, a reconstruction formula with Nyquist-type rate condition, similar to that in (1), is needed. We demonstrate that reconstruction formulas are relatively easy to find. However, methods used in frame theory [6, 26] and irregular sampling [11, 46] are necessary to establish these conditions.

Assuming that $(t_k), k \in \mathbb{Z}$, is a strictly increasing time sequence, a possible representation is given by

$$x(t) = \sum_{k\in\mathbb{Z}} c_k g(t - t_k), \tag{3}$$

where $g(t)$ is defined in (2) and the scalars c_k are to be determined. Evaluating both sides of (3) at $t = t_\ell$ gives

$$x(t_\ell) = \sum_{k\in\mathbb{Z}} c_k g(t_\ell - t_k), \tag{4}$$

or in matrix form

$$\mathbf{q} = \mathbf{G}\mathbf{c} \tag{5}$$

with unknown vector $[\mathbf{c}]_k = c_k$ and known vector $\mathbf{q}$ and matrix $\mathbf{G}$ given by:

$$[\mathbf{q}]_\ell = x(t_\ell), \quad \text{and} \quad [\mathbf{G}]_{\ell,k} = g(t_\ell - t_k). \tag{6}$$

It can be shown [19] that the unknown $\mathbf{c}$ can in principle be obtained from (5) if the average density of the t_k's is at or above the Nyquist rate, π/Ω. Therefore,

$$\max_k (t_{k+1} - t_k) \leq \frac{\pi}{\Omega} \tag{7}$$

is a sufficient condition for perfect reconstruction. The practical solution, however, is challenging because

- $\mathbf{G}$ is typically ill-conditioned,
- $\mathbf{q}$, $\mathbf{c}$, $\mathbf{G}$ should in principle have infinite dimensions.

In practice, only finite sets of the form $\{t_0, t_1, \ldots, t_{L-1}\}$ and $\{x(t_0), x(t_1), \ldots, x(t_{L-1})\}$ are available for recovery. Thus, $\mathbf{q}$ and $\mathbf{c}$ have L elements, $\mathbf{G}$ is an L by L matrix, and (5) becomes a finite set of linear equations. By solving these for $\mathbf{c}$, an approximate form of the signal is recovered (see also (3)):

$$x(t) \simeq \sum_{k=0}^{L-1} c_k g(t - t_k). \tag{8}$$

This approximation will be inaccurate outside (t_0, t_{L-1}) and close to the boundaries $t = t_0$ and $t = t_{L-1}$, but for reasonably large L a very good approximation can be achieved in a reduced range (t_M, t_{L-1-M}). Typically L and M takes values between 20-40 and 2-5, respectively. Since in this case the matrix $\mathbf{G}$ usually becomes ill-conditioned, a familiar (minimum-norm) solution is given by

$$\mathbf{c} = \mathbf{G}^{+}\mathbf{q}, \tag{9}$$

where $\mathbf{G}^{+}$ denotes the pseudo (Moore-Penrose) inverse of $\mathbf{G}$ [46, 3].

Finally, since the sufficient condition in (7) is valid for the infinite dimensional case only, it can merely be used as an indicator whenever finite-dimensional reconstructions are carried out.

2.2 Encoding Using Timing Information

Practical applications of irregular sampling are limited to a few areas including astronomical measurements, medical imaging, and the lost-data problem in communication theory [1]. The use of irregular sampling in communications is even more limited because of two main reasons. First, as mentioned in Section 2.1, the reconstruction of $\mathbf{c}$ based on (5) or (9) is difficult. Second, both the t_k's and the amplitude samples $x(t_k)$'s are needed for the reconstruction. Therefore, if the average density of the t_k's are at the Nyquist-rate, then two times as much information is needed for transmission when compared to regular sampling. Thus, in the regular sampling case, the t_k's carry no information and, therefore, do not need to be transmitted. Since apart from the fulfillment of the condition in (7) the t_k's can be arbitrary, appropriate circuits can set them such that the amplitude samples $x(t_k)$ take known values. In what follows circuits that represent amplitude information at the input as a time sequence at the output will be referred as Time Encoding Machines (TEMs).

2.2.1 Examples

Can the AADC of Figure 2 be used as a TEM? Although $x(t_k)$ certainly agrees with one of the quantization levels, additional information is needed to decide which one. Therefore, this circuit alone cannot be viewed as a TEM. An additional problem with this circuit is that the average density for the t_k's cannot be guaranteed. A signal dependent sampling mechanisms is required for this purpose.

A technique related to pulse position modulation (PPM) addresses this problem (see, e.g., [38]) using the circuit of Figure 3. Here the difference $x(t) - f(t)$ is passed through a comparator where $f(t)$ is a known function. As shown, the comparator fires at $t = t_k$ when $x(t_k) = f(t_k)$ holds. Clearly $x(t_k)$ no longer carries information since $f(t_k)$ is known. Therefore, the circuit in Figure 3 can be considered as a TEM. By properly choosing $f(t)$ (usually as a periodic ramp or sinusoid signal with appropriate amplitude and frequency) the condition in (7) can be satisfied. Although simple to implement, this circuit has not become popular in practical applications because it is highly sensitive to additive noise. Furthermore, VLSI implementations cannot guarantee the accurate shape of $f(t)$.

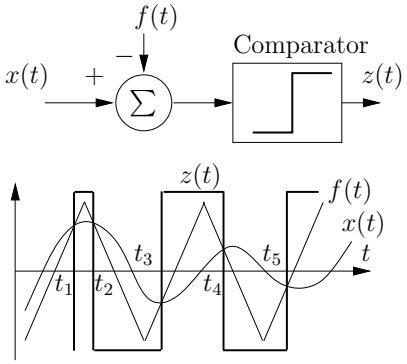

Figure 3: A simple TEM based on detecting zero-crossings.

2.3 Time Decoding Machines

Reconstruction algorithms corresponding to different TEMs can be formulated similarly to that for irregular sampling in Section 2.1. For example, the encoding mechanism in Figure 3 is similar to the one in irregular sampling except that $[\mathbf{q}]_\ell = f(t_\ell)$ is used as opposed to $[\mathbf{q}]_\ell = x(t_\ell)$.

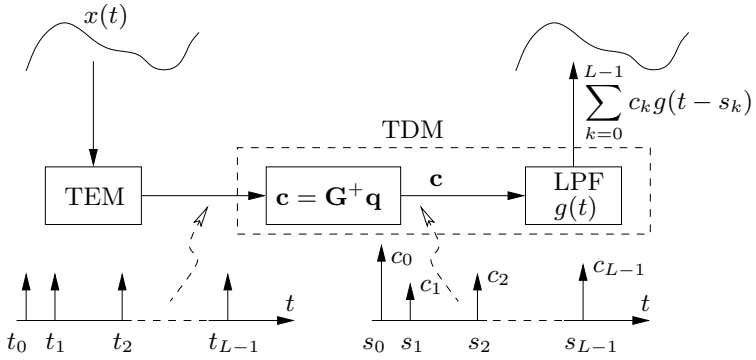

Figure 4: General reconstruction procedure.

All the reconstruction algorithms discussed in this paper call for solving a linear system of equations of the form (5). Overall, they implement the common scheme shown in Figure 4, where $\mathbf{q}$, $\mathbf{G}$ and the s_k's are TEM-dependent quantities. In what follows the t_k's will be referred to as time codes (TC) and will be represented by uniformly weighted pulses, as shown. Based on these TCs the vector $\mathbf{c}$ is calculated. Finally, the reconstructed signal is obtained by passing irregularly placed pulses weighted by the components of $\mathbf{c}$ through an ideal LPF. Subsequently, the overall reconstruction procedure will be referred to as a Time Decoding Machine (TDM). As in the irregular-sampling case, a TDM with a finite number of TCs gives an approximate reconstruction of the bandlimited signal.

Adopting the methods of irregular sampling [12, 46] alternative reconstruction procedures have been developed for the TEM discussed in Section 3. In [30] $\mathbf{G}$ was transformed into

a set of tridiagonal matrices after appropriate preconditioning. This solution is suitable for parallel processing via cellular neural networks (CNNs). With a different approach the computational load for calculating the pseudo inverse was reduced by transforming the linear equations describing the TEM into a Toeplitz system [32].

Finally we note that the TDM of Figure 4, those in [30, 32], and even the reconstruction methods for irregular sampling [12, 46] are off-line techniques since $x(t)$ can only be recovered if the TCs are known in a finite time interval. Real-time algorithms for the overall reconstruction based on stitching together finite-duration approximations will be presented elsewhere [35], [34].

2.4 Time Encoding Machines

The circuit in Figure 3 is a good example of an encoding mechanism that can be inverted by decodig techniques developed for the case of irregular sampling. An alternative is to use known robust circuits with low power consumption as TEMs and modify the corresponding TDMs appropriately. Fortunately, a number of potential TEMs exist among traditional circuits and those used in biomedical and biologically inspired applications. These TEMs are analog, nonlinear, and asynchronous circuits where the TCs can be identified by detecting zero-crossings, sharp transitions, or pulse positions of the TEM output, subsequently denoted by $z(t)$. Similarly to the discussion in Section 2.1, we shall see that the modified TDMs are relatively easy to find. Deriving validity conditions for these TDMs calls for methods used in irregular sampling and frame theory [31, 29] and will not be detailed here. These conditions can be viewed as quality indicators for implementable TDMs. Generally, larger margins for satisfying these conditions lead to better finite-dimensional approximations.

3 Asynchronous Sigma-Delta Modulator

The first example of a TEM [27, 31] was the asynchronous sigma-delta modulator [21, 42] shown in Figure 5. The TEM consists of integrator and a symmetrically-centered noninverting Schmitt trigger in a negative-feedback arrangement, where κ, δ and b are circuit parameters. As shown, the zero-crossings of the asynchronous binary output $z(t)$ define the

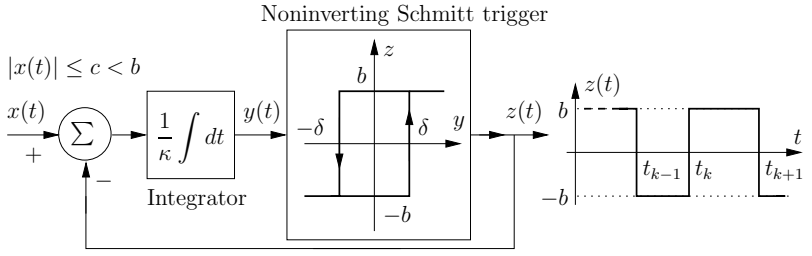

Figure 5: Asynchronous sigma-delta modulator as a TEM.

TCs. Furthermore, as also shown in the figure, the input signal is bounded in amplitude as:

$$|x(t)| \leq c < b. \tag{10}$$

3.1 Time Encoding

The operation of the TEM in Figure 5 is simple. Since $z(t)$ takes either b or $-b$ values, the input to the integrator is either $x(t)+b$ or $x(t)-b$. Then, due to (10) the integrator output, $y(t)$, is a strictly increasing or decreasing function for $t \in [t_k, t_{k+1}]$ so that $y(t_k) = (-1)^k\delta$ holds. A straightforward analysis [31] gives

$$\int_{t_k}^{t_{k+1}} x(t)dt = (-1)^k(2\kappa\delta - b(t_{k+1} - t_k)), \tag{11}$$

for all k. Using (11) and (10) it can be shown [31] that the difference between the neighboring TCs is bounded as

$$\frac{2\kappa\delta}{b+c} \leq t_{k+1} - t_k \leq \frac{2\kappa\delta}{b-c}. \tag{12}$$

3.1.1 Example

Let $x(t)$ be given by the familiar sampling representation in (1) where $\Omega = 2\pi \times 40$ kHz, $T = \pi/\Omega = 12.5$ μs is the Nyquist-period. A finite set of samples were randomly chosen as $x(T) = -0.1961$, $x(2T) = 0.186965$, $x(3T) = 0.207271$, $x(4T) = 0.0987736$, $x(5T) = -0.275572$, $x(6T) = 0.0201665$, $x(7T) = 0.290247$, $x(8T) = 0.138374$, $x(9T) = -0.067588$, $x(10T) = -0.145661$, $x(11T) = -0.11133$, $x(12T) = -0.291498$. The rest of the samples were set to zero, i.e., $x(kT) = 0$ for $k \leq 0$ and $k12$. The evaluation of the TCs was carried out in the interval $-2T \leq t \leq 15T$ by the recursive numerical solution of the TEM equation in (11). Here t_{k+1} is obtained in terms of t_k. During the numerical simulations the accuracy was set to high precision. Figure 6 shows portions of the input $x(t)$ (black solid line), the integrator output $y(t)$ (dashed line), and the asynchronous binary TEM output $z(t)$ (solid gray line).

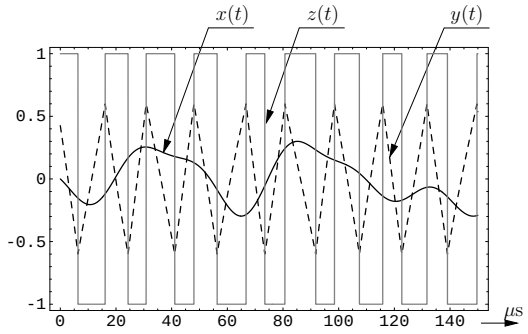

Figure 6: Simulation results for the signals in Fig. 5.

3.2 Time Decoding

The original TDM of [27] can be found by assuming $x(t)$ to be of the form of

$$x(t) = \sum_{\ell \in \mathbb{Z}} c_\ell g(t - s_\ell) \quad \text{with} \quad s_\ell = \frac{t_\ell + t_{\ell+1}}{2}, \tag{13}$$

and the unknown coefficients c_ℓ. Substituting (13) into (11) gives:

$$\sum_{\ell \in \mathbb{Z}} c_\ell \int_{t_k}^{t_{k+1}} g(t - s_\ell) dt = (-1)^k (2\kappa\delta - b(t_{k+1} - t_k)). \tag{14}$$

Therefore, with vector $\mathbf{q}$ and matrix $\mathbf{G}$ given by

$$\begin{aligned} [\mathbf{q}]_k &= (-1)^k (2\kappa\delta - b(t_{k+1} - t_k)) \\ \text{and} \quad [\mathbf{G}]_{k,\ell} &= \int_{t_k}^{t_{k+1}} g(t - s_\ell) dt, \end{aligned} \tag{15}$$

$\mathbf{Gc} = \mathbf{q}$ and hence the TDM of Figure 4. It can be shown [31] that (7) serves as a sufficient condition for perfect reconstruction (with infinite dimensional $\mathbf{q}$ and $\mathbf{G}$). Combining (7) with (12) gives the sufficient condition

$$\frac{2\kappa\delta}{b - c} < \frac{\pi}{\Omega} \tag{16}$$

in terms of the circuit parameters κ, δ, and b, and the amplitude and frequency bounds of the input, c and Ω, respectively.

3.2.1 Time Quantization

In addition to the reconstruction error due to the finite dimensionality of $\mathbf{q}$ and $\mathbf{G}$, an error certainly shows up whenever the TCs are available with finite precision or in quantized form. In practice, the bounds in (12) makes the quantization of the TCs straightforward. If $2\kappa\delta/(b + c)$ is known, then only the difference of the upper and lower bound in (12) needs to be represented by as quantizer. Thus, if N bits are used for time quantization, then the corresponding error in representing $t_{k+1} - t_k - 2\kappa\delta/(b + c)$ is in the range:

$$\Delta = \frac{1}{2^N} \left(\frac{2\kappa\delta}{b - c} - \frac{2\kappa\delta}{b + c} \right) = \frac{2\kappa\delta}{2^N} \frac{2c}{b^2 - c^2}.$$

The quantization of $t_{k+1} - t_k - 2\kappa\delta/(b + c)$ can be implemented by a single clock with frequency $1/\Delta$ started at t_k and stopped after the appearance of t_{k+1}. From these quantized TC values the matrix $\mathbf{G}$ can easily be calculated.

In [31] the effect of time quantization was investigated in detail. An upper bound and an approximation for the corresponding reconstruction error was developed and confirmed

by simulations. As shown in [31], unless N is very large, the error due to time-quantization can easily dominate over the error due to the finite dimensionality of $\mathbf{q}$ and $\mathbf{G}$. In addition, doubling the time-quantizing clock, hence increasing the number of bits by one, decreases the root-mean-square (RMS) reconstruction error by about 6 dB. The same well-known result holds for amplitude quantization, when the number of quantization levels is doubled. This improvement, however, is far below the one obtained with clocked sigma-delta modulators, where doubling the clock frequency improves the (in-band) reconstruction error by 9-15 dB [40].

3.2.2 Example

Using the parameters of Section 3.1.1 with $L = 26$ the TCs (only 18 TCs are shown in Fig. 6) were determined with high accuracy. Defining the error function $e(t)$ as the difference between the reconstructed signal and $x(t)$, simulation results based on using accurate and quantized to N bits TCs are shown in Figure 7. Here $\mathcal{E}$ denotes the RMS value of $e(t)$ evaluated over the time interval shown in the figure. In agreement with Section 3.2.1, this example demonstrates that increasing N by one, decreases the reconstruction error by about 6 dB. Indeed, considering the case $N = 14$ we have -97 dB $- 6 \times 6$ dB $= -133$ dB which is close to simulated result for $\mathcal{E}$ shown with $N = 20$.

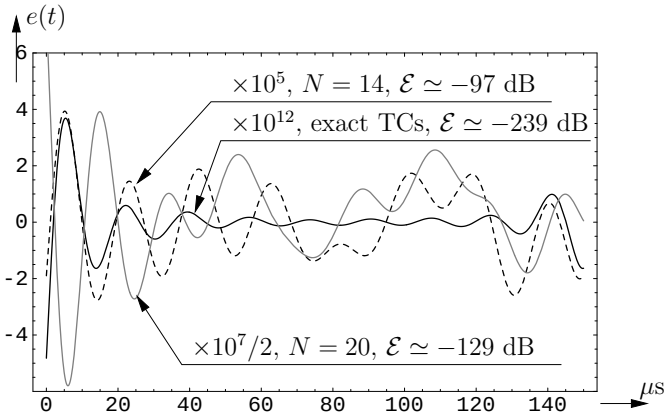

Figure 7: Simulation results for the error function with perfect TCs and those quantized to $N = 14$ and $N = 20$ bits.

3.3 Parameter-Insensitive Reconstruction

From (15) it can be seen that the reconstruction depends on the circuit parameters κ, δ and b. If time encoding is used in communications and the TEM is at the transmitter side, then these parameters are not necessarily known by the receiver (TDM). This parameter-dependency can easily be eliminated in several ways [31] . For example, adding (14) for $k = m$ and $k = m + 1$ gives:

$$\sum_{\ell\in\mathbb{Z}} c_\ell \left(\int_{t_m}^{t_{m+1}} g(t-s_\ell)dt + \int_{t_{m+1}}^{t_{m+2}} g(t-s_\ell)dt \right) = (-1)^m b(t_{m+2} - 2t_{m+1} + t_m).$$

Therefore, with

$$\begin{aligned} [\mathbf{G}]_{m,\ell} &= \int_{t_m}^{t_{m+2}} g(t-s_\ell)dt \\ \text{and} \quad [\mathbf{q}]_m &= (-1)^m b((t_{m+2} - 2t_{m+1} + t_m)), \end{aligned}$$

$x(t)$ can be reconstructed up to a scaling factor b. The condition (16) remains valid [31] for this reconstruction algorithm as well.

3.4 VLSI Considerations

In [22] the robustness in performance of the TDM was investigated when the TEM is subject to non-idealities of the analog VLSI realization. The integrator was implemented as a simple one-opamp active RC circuit with an input-referred offset voltage, finite DC gain, and finite bandwidth for the opamp. In addition, parameter errors were assumed for the centering of the Schmitt trigger. An analysis confirmed by numerical simulations showed [22] that the input signal can be accurately reconstructed even in the presence of these errors. In particluar it was shown that

- the parameter-insensitive reconstruction in Section 3.3 is insensitive with respect to the horizontal-centering error of the Schmitt-trigger characteristic;
- the offset voltage of the opamp and the vertical-centering error of the Schmitt-trigger characteristic introduces merely a constant DC error in the reconstructed signal;
- reasonably large values for the DC gain and bandwidth of the opmap results in a constant delay error in the reconstructed signal.

This type of robustness is similar to that of sigma-delta modulators. Indeed, replacing the Schmitt trigger by a clocked quantizer results in the familiar first-order, single-bit, single-loop [40] sigma-delta modulator.

4 Alternative Time Encoding Machines

Here we illustrate that existing well-known circuits can be employed as TEMs. That is, independently of their conventional use, they can be viewed as information-processing modules that make possible perfect reconstruction of a bandlimited signal based on timing information only.

4.1 Frequency Modulation

Frequency modulation (FM) [2] traditionally consists of a FM modulator and an FM demodulator. The FM modulator produces the signal

$$z(t) = \sin\left(f(t)\right) \quad \text{with} \quad f(t) = \omega t + \eta \int_{t_0}^{t} x(u)du + \phi, \tag{17}$$

where ω is the modulation frequency (carrier rate), η is the modulation index (modulation gain), and ϕ is an initial phase. The FM demodulator recovers the information-carrying signal $x(t)$ from $z(t)$ using well-known techniques.

Let us now consider the zero-crossings of the output of the FM modulator $z(t)$ [31]. First, $z(t_1) = 0$ holds for the smallest $t_1 > t_0$, when $f(t_1) = \pi$. Similarly, $z(t_2) = 0$ holds for the smallest $t_2 > t_1$, when $f(t_2) = 2\pi$. Therefore, in general $f(t_k) = k\pi$ must hold. In this way we have $f(t_{k+1}) - f(t_k) = \pi$. Rearranging this relationship using (17) gives:

$$\int_{t_k}^{t_{k+1}} x(u)du = \frac{\pi}{\eta} - \frac{\omega}{\eta}(t_{k+1} - t_k).$$

This formulations has the same structure as that in (11). Therefore, the reconstruction of Section 3.2 can be used with the same $\mathbf{G}$ and:

$$[\mathbf{q}]_k = \frac{\pi}{\eta} - \frac{\omega}{\eta}(t_{k+1} - t_k).$$

4.2 Spiking Neurons

Spiking neurons with pulse-train outputs are well-known modules in biomedical engineering and neural networks. They are closely related to biological neurons, see, e.g., [13]. The ideal integrate-and-fire (IAF) and leaky IAF neuron model produces an analog cell potential based on linearly filtering synaptic inputs. Whenever the cell potential exceeds a fixed threshold level, a discrete action potential is generated. For example, the IAF neuron with time-varying threshold is used to model the sino-atrial node of the heart [44].

4.2.1 IAF Neuron with a Refractory Period

The operational properties of an IAF neuron can be described by the circuit shown in Figure 8. The input signal is biased by b and, as shown, (10) holds. Therefore the integrator output $y(t)$ is an increasing signal. When $y(t)$ reaches δ, the integrator is initialized and a pulse is produced at the overall output. A fixed amount of time, Δ (refractory period), is assumed for integrator initialization and pulse production. From simple circuit equations we have:

$$\int_{t_k+\Delta}^{t_{k+1}} x(u)du = \kappa\delta - b(t_{k+1} - t_k - \Delta)$$

The analysis of this circuit [29] gives the following results.

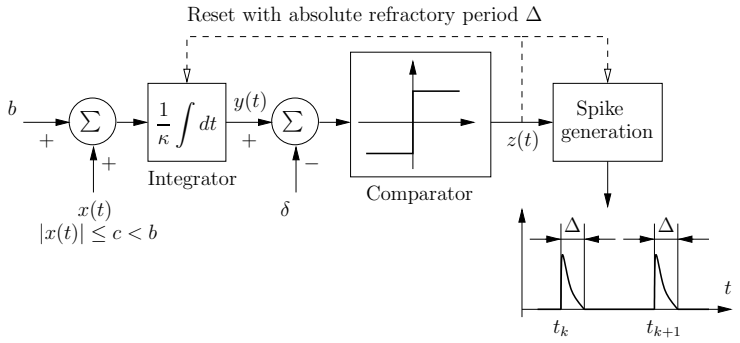

Figure 8: Operational model for an integrate-and-fire neuron.

- The neighboring TCs are bounded as

$$\frac{\kappa\delta}{b+c} + \Delta \leq t_{k+1} - t_k \leq \frac{\kappa\delta}{b-c} + \Delta,$$

  similarly to (12).

- With s_k defined in (13) the TDM of Figure 4 applies with

$$\begin{aligned} [\mathbf{q}]_k &= \kappa\delta - b(t_{k+1} - t_k - \Delta) \\ \text{and} \quad [\mathbf{G}]_{k,\ell} &= \int_{t_k+\Delta}^{t_{k+1}} g(t - s_\ell)dt. \end{aligned}$$

- Perfect reconstruction (with infinite dimensional $\mathbf{q}$ and $\mathbf{G}$) can be achieved if

$$\frac{\kappa\delta}{b-c} + \Delta < \frac{1+\varepsilon}{1-\varepsilon}\frac{\pi}{\Omega} \quad \text{where} \quad \varepsilon = \frac{\Delta}{\Delta + \frac{\kappa\delta}{b+c}}.$$

4.2.2 Multichannel Extensions

The extension to leaky IAF neurons was investigated in [33]. In the same paper leaky IAF neurons were used to represent $x(t)$ by multidimensional spike trains. A canonical model was derived by first processing $x(t)$ with an analog filter bank. Then, the filter outputs were processed by separate TEMs producing individual sets of spike trains. The canonical TEM can be used to model a number of sensory systems including retina [39] and cochlea [17]. In [33] it was proven that this multichannel time encoding machine is invertible under certain natural conditions. That is, a sensory stimulus can be recovered from its multidimensional spike-train representation without loss of information.

4.2.3 CMOS Considerations

The possibility of accurate reconstruction from spiking neuron circuits and the high-level implications of time encoding in general was recognized in [8, 5]. In [8] SPICE simulations

of CMOS spiking neurons were used to demonstrate that 12-bit precision can be achieved if these neurons are used as ADCs. The input signal was a Gaussian random noise (similar to that used in Section 3.2.2) with bandwidth $\Omega = 3000\pi$, and the time-quantizing clock (see Section 3.2.1) was 1 MHz. In [5] a bio-amplifier with pulse output was discussed. It was shown that the circuit fabricated by a 0.6 μm CMOS process achieved a gain of 39.5 dB between 0.3 Hz and 5.4 kHz so that, as a detailed analysis on power budget showed in [5], the total power consumption was less than 0.3 mW.

4.3 Time Encoding and Decoding with Erasures

Time encoding is closely related to frame theory [31, 29]. Recently it has been shown [4] that even smaller subsets of frames often preserve the key frame properties. In addition, the redundancy of the frame representation can be used even when some information is lost during transmission. Representations based on frames and thereby, time encoding and decoding processing exhibit resilience to additive noise as well as numerical stability in real-time reconstruction. As in the case of improving Internet packet losses [14] and filter bank implementations [26], an exchange algorithm can be devised for protecting the time encoded signal at the receiver side (TDM) even in the absence of some of the timing information. Preliminary investigations show that a substantial number of time codes can be discarded while TDM recovery algorithms provide acceptable recovery results. Clearly, the recovery depends on the average density of the time codes [19]. This can be viewed as an inherent error-correcting mechanism for the time encoding-decoding process against data corruption during transmission.

5 Conclusions and Future Work

Time encoding is an alternative modality for representing the information carried by bandlimited signals. The information is carried by timing information (time codes) based on which the signal can be (in principle) perfectly reconstructed. As opposed to the Shannon-Nyquist type of synchronous (clock-based) amplitude-sampling, time encoding is an asynchronous mechanism.

Known analog, nonlinear, asynchronous, and low-power circuits can be used as time encoders (TEMs) at the price of more intensive reconstruction procedures. Its most probable potentials are in power-critical applications such as sensor-networks [41], human-area or body-area networks, or in "mobile computing, medical sensor, and communication technologies for health-care" commonly referred to as M-Health [18]. In these areas the lifetime of the self-powered sensors is extremely important, whereas the reconstruction can be carried out at some remote site where the required power and computational infrastructure is available.

From the transmission point of view, the asynchronous binary signals or pulse-trains of TEM output exhibit the same type of immunity against noise and crosstalk as the commonly-used synchronous digital signals. An important problem here is to find the most appropriate transmission system. For reconstructing the signal, the time codes must eventually have

numerical values. However, whether time quantization should be implemented at the transmitter before modulation, at the receiver after demodulation, or at some intermediate point, remains an open question. Finding modulation schemes that are best suited for asynchronous spikes or binary signals are an area under active investigation.

An important goal is to find efficient reconstruction procedures. Real-time recovery [35], [34], for example, is an enabler of real-time monitoring in M-Health applications. Offline reconstruction algorithms, such as the TDM presented in this paper, can be used for interpreting recorded spike trains generated by real biological neurons. The interpretation, of course, depends on the reliability of the model.

References

[1] A. Aldroubi and K. Gröchenig, "Non-uniform sampling and reconstruction in shift-invariant spaces", *SIAM Review*, Vol. 43, pp. 585-620, 2001.

[2] E. H. Armstrong, "A Method for reducing disturbances in radio signaling by a system of frequency modulation", *Proceedings of Institute of Radio Engineers*, Vol. 24, No. 5, May 1936.

[3] S. L. Campbell and C. D. Meyer, Jr: *Generalized Inverses of Linear Transformations*, Dover Publications, 1979.

[4] P.G. Casazza, "The art of frame theory", *Taiwanese J. of Math.* 4 (2000), pp. 129-201.

[5] D. Chen, J. G. Harris and J. C. Principe, "A bio-amplifier with pulse Output", *Proc. of the 26th Annual International Conference of the IEEE EMBS*, San Francisco, CA, USA, September 1-5, 2004, pp. 4071- 4074.

[6] O. Christensen, *Frames Riesz basis, and discrete Gabor/wavelet expansions*, Bulletin (New York) of the American Mathematical Society, Vol. 38, No. 3, pp. 273-291, March 27, 2001.

[7] M. Conti, S. Orcioni, C. Turchetti, and G. Biagetti, "A current mode multistable memory using asynchronous successive approximation A/D converters", *International Conference on Electronics, Circuits and Systems, IEEE*, 1999, pp. 513-516.

[8] W. Dazhi and J. G. Harris,"Signal reconstruction from spiking neuron models", *Proceedings of the 2004 International Symposium on Circuits and Systems* Vancouver, Canada, Vol. 5, 23-26 May pp. 616 - 618, 2004.

[9] R. J. Duffin and A. C. Schaeffer, "A class of nonharmonic Fourier series", *Transactions of the American Mathematical Society*, Vol. 72, pp. 341-366, 1952.

[10] K. M. Fant and S. A. Brandt, "NULL convention logic: a complete and consistent logic for asynchronous digital circuit synthesis", *International Conference on Application Specific Systems, Architectures, and Processors*, pp. 261-273, 1996.

[11] H. G. Feichtinger and K. Gröchenig, *Theory and Practice of Irregular Sampling*. In J.J. Benedetto and M.W. Frazier, editors, Wavelets: Mathematics and Applications, pp. 305-363, CRC Press, Boca Raton, FL, 1994.

[12] H. G. Feichtinger, K. Gröchenig, and T. Strohmer, "Efficient numerical methods in non-uniform sampling theory", *Numerische Mathematik*, 69:423-440, 1995.

[13] W. Gertner and W. Kistler, *Spiking Neuron Models, Single Neurons, Populations, Plasticity*, Cambrdige University Press, 2002.

[14] V.K. Goyal, J. Kovacevic and J.A. Kelner, "Quantized frame expansions with erasures", *Applied and Computational Harmonic Analysis (ACHA)*, Vol. 10, No. 3, (2001), pp. 203-233.

[15] G. R. Harris and T. Kocak, "A novel asynchronous ADC architecture", *Proceedings of the IEEE 11th Annual NASA Symposium on VLSI Design*, Coeur d'Alene, ID, 2003.

[16] A. Hemani, T. Meincke, S. Kumar, A. Postula, T. Olsson, P. Nilsson, J. Oberg, P. Ellervee, and D. Lundqvist, "Lowering power consumption in clock by using globally asynchronous locally synchronous design style," *Proceedings of the 36th ACM IEEE conference on Design automation table of contents*, New Orleans, Louisiana, USA, pp. 873 - 878, 1999.

[17] A.J. Hudspeth, M. Konishi, "Auditory neuroscience: development, transduction and integration", *Proc. Natl. Acad. Sci.* USA 97 (22) (2000) 11690-11691.

[18] R. S. Istepanian, E. Jovanov, and Y. T. Zhang, "Introduction to the special section on M-Health:beyond seamless mobility and global wireless health-care connectivity,", Guest Editorial, *IEEE Transactions on Information Technology in Biomedicine*, Vol. 8, No. 4, pp. 405-413, December 2004.

[19] S. Jaffard, "A density criterion for frames of complex exponentials", *Michigan Mathematical Journal*, Vol. 38, No. 3, pp. 339-348, 1991.

[20] P. W. Jungwirth and A. D. Poularikas, "Improved Sayiner level crossing ADC," *Proceedings of the Thirty-Sixth Southeastern Symposium on System Theory*, 2004, pp. 379 - 383.

[21] C. J. Kikkert, and D. J. Miller,' 'Asynchronous delta sigma modulation", *Proceedings of the IREE (Australia)*, Vol. 36, pp. 83-88, April 1975.

[22] P. R. Kinget, A. A. Lazar, and L. T. Tóth, "On the robustness of the VLSI implementation of a time encoding machine," *Proceedings of ISCAS 2005*, pp. 4221-4224, May 23-26, 2005, Kobe, Japan.

[23] D.J. Kinniment, B. Gao, A.V. Yakovlev, and F. Xia, "Towards asynchronous A-D conversion", *Fourth International Symposium on Advanced Research in Asynchronous Circuits and Systems*, pp. 206 -215, 1998.

[24] D.J. Kinniment, A.V. Yakovlev, and B. Gao, "Synchronous and asynchronous A-D conversion", *IEEE Transactions on Very Large Integration Systems*, Vol. 8, No. 2, pp. 217-220, April 2000.

[25] V.A. Kotel'nikov, *On the Transmission Capacity of the Ether and Wire in Electrocommunications*, In J.J. Benedetto and P.J.S.G. Ferreira, editors, Modern Sampling Theory, Mathematics and Applications, pp. 27-45. Birkhauser, Boston, MA, 2001. Translated by V.E. Katsnelson from the Russian original published in Izd. Red. Upr. Suyazi RKKA, Moscow 1933.

[26] J. Kovačević, P.L. Dragotti and V.K. Goyal, "Filter bank frame expansions with erasures", Invited Paper, *IEEE Transactions on Information Theory*, Vol. 48, No. 6 pp. 1439-1450, June 2002.

[27] A.A. Lazar and L.T. Tóth, "Time encoding and perfect recovery of bandlimited signals", *Proceedings of the ICASSP'03*, Vol. VI, pp. 709-712, April 6-10 2003, Hong Kong.

[28] A.A. Lazar, "Time Encoding: A Novel Signal Processing Paradigm for Ulta-Low Voltage Applications ," *Invited Speaker at the Conference on Nanotechnology*, Budapest, Hungary, April 26-27, 2004.

[29] A.A. Lazar, "Time encoding with an integrate-and-fire neuron with a refractory period", *Neurocomputing*, Vol. 58-60, pp 53-58, June 2004.

[30] A.A. Lazar, T. Roska, E.K. Simonyi and L.T. Tóth, L.T., "A Time decoding realization with a CNN," *Proceedings of Neurel 2004*, pp. 97-102, September 23-25, 2004, Belgrade.

[31] A.A. Lazar and L.T. Tóth, "Perfect recovery and sensitivity analysis of time encoded bandlimited signals, *IEEE Transactions on Circuits and Systems-I: Regular Papers*, Vol. 51, No 10, pp. 2060-2073, October 2004.

[32] A.A. Lazar, E.K. Simonyi and L.T. Tóth, "Fast recovery algorithms of time encoded bandlimited signals," *Proceeding of the International Conference on Acoustics, Speech and Signal Processing (ICASSP'05)*, Philadelphia, PA, March 19-23, 2005, Vol. 4, pp. 237-240, 2005.

[33] A.A. Lazar, "Multichannel time encoding with integrate-and-fire neurons", *Neurocomputing*, Vol. 65-66, pp. 401-407, June 2005.

[34] A.A. Lazar, E.K. Simonyi, and L.T. Tóth, "A Toeplitz formulation of a real-time algorithm for time decoding machines," Proceedings of the *International Conference on Telecommunication Systems, Modeling and Analysis (ICTSM'05)*, Dallas, TX, November 17-20, 2005.

[35] A.A. Lazar, E.K. Simonyi, and L.T. Tóth, "An real-time algorithm for time decoding machines," *BNET Technical Report #4-05*, Department of Electrical Engineering, Columbia University, New York, October 2005.

[36] Y. Li, G. Patounakis, K.L. Shepard, and S.M. Nowick, "Design of an asynchronous micropipelined datapath with heterogeneous, dynamic voltage scaling," *IEEE Journal of Solid-State Circuits*, April, 2004.

[37] A. J. Martin, M. Nystrom, and C.G. Wong, "Three generations of asynchronous microprocessors", *Design and Test of Computers, IEEE*, Vol. 20, No. 6, Nov.-Dec. 2003, pp. 9-17.

[38] F. Marvasti and M. Sandler, *Applications of Nonuniform Sampling to Nonlinear Modulation, A/D and D/A Techniques*. In F. Marvasti, editor, Nonuniform Sampling, Theory and Practice, pp. 647-687, Kluwer Academic/Plenum Publishers, New York, 2001.

[39] R.H. Masland, "The fundamental plan of the retina", *Nat. Neurosci.* 4 (9) (2001) 877-886.

[40] S.R. Norsworthy, R. Schreier, and G.C. Temes (editors), *Delta-Sigma Data Converters*, IEEE Press, New York, 1997.

[41] D. Pucinelli and M. Haenggi, "Wireless sensor networks: applications and challenges of ubiquitous sensing", *IEEE Circuits and Systems Magazine*, Vol. 5, No. 3, pp. 19-29, 2005.

[42] E. Roza, "Analog-to-digital conversion via duty-cycle modulation", *IEEE Transactions on Circuits and Systems-II: Analog and Digital Signal Processing*, Vol. 44, No. 11, pp. 907-917, November 1997.

[43] N. Sayiner, H.V. Sorensen, and T.R. Viswanathan," A level-crossing sampling scheme for A/D conversion," *IEEE Transactions on Circuits and Systems II: Analog and Digital Signal Processing*, Vol. 43, No. 4, pp. 335-339, 1996.

[44] S.R. Seydnejad and R.I. Kitney, "Time-varying threshold integral pulse frequency modulation", *IEEE Transactions on Biomedical Engineering*, Vol. 48, No. 9, pp. 949-962, September 2001.

[45] C.E. Shannon, "Communications in the presence of noise," *Proceedings of the IRE*, Vol. 37, pp. 10-21, January 1949.

[46] T. Strohmer, *Irregular Sampling, Frames, and Pseudoinverse*, Master thesis, Dep. Math. Univ. Vienna, Austria, 1993.

[47] S. H. Unger, "Reducing power dissipation, delay, and area in logic circuits by narrowing transistors," *Design and Test of Computers, IEEE*, Vol. 20, Issue 6, Nov.-Dec. 2003, pp. 18-25.

[48] R. M. Young, *Introduction to Nonharmonic Fourier Series*, Academic Press, New York, 1980.